Kinematic simulation of turbulent dispersion of triangles

M. A. I. Khan,[1,*] A. Pumir,[2] and J. C. Vassilicos[3]

[1]*DAMTP, University of Cambridge, Silver Street, Cambridge CB3 9EW, United Kingdom*
[2]*INLN, 1361 route des Lucioles, F-06560, Valbonne, France*
[3]*Department of Aeronautics, Imperial College, London SW7 2BY, United Kingdom*

As three particles are advected by a turbulent flow, they separate from each other and develop nontrivial geometries, which effectively reflect the structure of the turbulence. We investigate here the geometry, in a statistical sense, of three Lagrangian particles advected, in two dimensions, by kinematic simulation (KS). KS is a Lagrangian model of turbulent diffusion that makes no use of any δ correlation in time at any level. With this approach, situations with a very large range of inertial scales and varying persistence of spatial flow structure can be studied. We first demonstrate that the model flow reproduces recent experimental results at low Reynolds numbers. The statistical properties of the shape distribution at a much higher Reynolds number is then considered. The numerical results support the existence of nontrivial shape statistics, with a high probability of having elongated triangles. Even at the highest available inertial range of scales, corresponding to a ratio between large and small scale $L/\eta = 17\,000$, a perfect self-similar regime is not found. The effects of the parameters of the synthetic flow, such as the exponent of the spectrum and the effect of the sweeping affect our results, are also discussed. Special attention is given to the effects of persistence of spatial flow structure.

PACS number(s): 47.27.Qb

I. INTRODUCTION

The transport of scalar fields by turbulent flows is an important process in many physical situations ranging from the dynamics of the atmosphere and the ocean to chemical engineering. Specific examples of scalars are provided by pollutant density, temperature or humidity fields, and the concentration of chemical and biological species [1].

Issues of transport and mixing in turbulence are directly related to the properties of fluid trajectories. The problem is thus often addressed using Lagrangian techniques [2–4]. There is an established formal connection between the statistics of fluid particle motion and the concentration field of a diffusing scalar [5]. Hence, the important modeling issue of predicting passive scalar transport in turbulence can be addressed by following the evolution of Lagrangian particles [2–4].

The dispersion problem of one or two particles in the flow has been studied in great detail. In particular, the seminal work of Richardson [6] leads to the prediction that the separation between two particles grows according to $\langle R^2 \rangle \propto \varepsilon t^3$, where ε is the rate of energy dissipation in the flow. Much less work has been devoted to the dispersion of three or more particles. The remarkable organization of the flow, which leads to the formation of very sharp fronts of scalar concentration [7–10], has a nontrivial signature on the three-point correlation function of the flow [11–13]. This, together with the well-established relation between the properties of the n-point correlation function and the properties of the evolution of n fluid particles advected by the flow, provides the motivation for studying the problem of dispersion of three

particles or more. Despite recent progress both theoretically [14,20] and experimentally [15–18], little is known about the dispersion of three particles or more.

An extra motivation to study dispersion of more than two particles comes from recent theoretical attempts to model turbulent velocity fluctuations in terms of small sets of Lagrangian particles [19,20].

The evolution of three particles configuration in turbulent flows has been considered numerically in direct numerical simulations (DNS) of three-dimensional (3D) flows, at moderate Reynolds number [21]. Because of the limited range of inertial scales available in DNS, the numerical studies are unable to answer questions about shape statistics in the inertial range. A phenomenological model, introduced to describe the shape deformation in the inertial range, in high Reynolds number flows, leads to the prediction of a nontrivial shape distribution [21]. This model provided both the motivation and the theoretical background to analyze the experimental results of Ref. [22]. This experiment provided important insight on the statistics of deformation, although the experimental setup also suffered from the limited inertial range.

In this paper, we consider the problem of Lagrangian dispersion of three particles with the help of the kinematic simulation (KS) method, introduced in Ref. [23]. The KS provides a Lagrangian model of turbulent diffusion, based on a simplified incompressible velocity field, with a proper energy spectrum and no assumption of δ correlation in time made at any level. This model reproduces very well the Lagrangian properties observed in laboratory experiments [24], as well as in DNS [25]. The computational simplicity of the KS allows us to consider very large inertial ranges: a ratio of scales of $\sim 10^4$ is easily accessible with moderate computer resources. The KS thus turns out to be a powerful tool to study issues of dispersion in turbulent flows.

The present work is devoted to the study of triangles, in a

---

*Present address: MCND, Department of Physics, University of Manchester, Oxford Road, Manchester M13 9PL, United Kingdom. Email address: amir@reynolds.ph.man.ac.uk

68 026313-1

two-dimensional flow, by using KS. The choice of a two-dimensional flow allows us to make direct comparisons with the available experimental data at low Reynolds numbers. We first demonstrate that KS effectively reproduces the experimental results of Ref. [22]. However, the experimental setup also suffers from the limited inertial range, thus shedding no light on the shape distribution in the case of high Reynolds number flows.

The main aim of this work is to investigate the shape distribution of triangles advected by a turbulent flow with a large Reynolds number using KS. The prediction of a nontrivial shape distribution [21] was based on a rather phenomenological model, and thus contains possibly questionable assumptions. Neither the numerical nor the experimental available results allow us to draw definite conclusions on shape statistics at large Reynolds numbers. We demonstrate here the existence of a nontrivial shape statistics of triangles advected by KS when the inertial range of scales is large (with an aspect ratio as high as $L/\eta = 17\,000$, where L and η are the large and small scale cutoffs of the energy spectrum's power-law shape). Qualitatively, our results show that the hierarchy of scales present in the flow leads to a non-Gaussian shape distribution for a triangle, in agreement with the phenomenological prediction of Ref. [21]. This is the main result of this work. Although the KS study does not allow us to make definite predictions about the problem of dispersion by a "real" turbulent flow, it is highly suggestive that a similar effect should exist in real flows.

In Sec. II, we briefly discuss the parametrization used to characterize the size and shape of the triangles, and we review the theoretical and experimental results on shape dynamics. Technical aspects of the simulation methods are described in Sec. III. The comparison between the experimental results of Ref. [22] and the KS simulations are presented in Sec. IV. Section V contains our results concerning the large Reynolds number limit. In Sec. VI we discuss the effects of persistence of flow structures on shape dynamics. Last, we present our concluding remarks in Sec. VII.

II. PREVIOUS RESULTS ON SHAPE DYNAMICS

In this section, we briefly review the previous work on shape dynamics [21,22].

A. Kinematics

The evolution of a cluster of particles is described both by the overall scale and by the shape of the object. In the case of a set of $n=3$ particles, located at x_i ($i=1,2,3$), we define a set of reduced vectors involving relative separations only, defined by Refs. [11,12]:

$$\boldsymbol{\rho}_1 = \frac{(x_2 - x_1)}{\sqrt{2}}, \tag{2.1}$$

$$\boldsymbol{\rho}_2 = \frac{(2x_3 - x_2 - x_1)}{\sqrt{6}}. \tag{2.2}$$

The radius of gyration is defined as [11]

$$R^2 = \sum_{i=1}^{2} \boldsymbol{\rho}_i^2 = \frac{1}{3} \sum_{jk} r_{jk}^2, \tag{2.3}$$

where $r_{ij}^2 = |x_i - x_j|^2$ are the distances between the vertices of the triangle. The quantity R measures the spatial extent of the swarm of particles. In order to characterize the shape, we introduce a moment of inertia like tensor [21]

$$g^{ab} = \sum_{i=1}^{2} \rho_i^a \rho_i^b, \tag{2.4}$$

where ρ_i^a is the ath spatial component of the vector $\boldsymbol{\rho}_i$. For a triangle in two dimensions, the tensor g has two eigenvalues, $g_1 > g_2$ (note that $g_1 + g_2 = R^2$). These eigenvalues characterize the spatial extent of the swarm in the two principal directions. The ratio I_2 between the smallest eigenvalue g_2 and R^2,

$$I_2 = \frac{g_2}{R^2}, \tag{2.5}$$

provides us with a quantitative measure of the shape of the object. An equilateral triangle corresponds to $I_2 = 1/2$. The smaller the I_2, the more elongated the triangle is. The moment of inertia tensor can be used both in two and three dimensions to characterize a set consisting of an arbitrary number of particles.

In the case of a triangle, a full parametrization of the shape is provided by the quantities w and χ, defined by

$$\chi = \frac{1}{2}\arctan\left[\frac{2\boldsymbol{\rho}_1 \cdot \boldsymbol{\rho}_2}{\rho_1^2 - \rho_2^2}\right], \quad w = 2\frac{|\boldsymbol{\rho}_1 \times \boldsymbol{\rho}_2|}{R^2}. \tag{2.6}$$

By taking into account the symmetries of the triangle under any reparametrization of its vertices, the parameter space is restricted to $0 \leq w \leq 1$ and $0 \leq \chi \leq \pi/6$. The variables w and I_2 are related by the relation, $I_2 = (1/2)(1 - \sqrt{1 - w^2})$. A small value of w corresponds to a nearly collinear set of points. The quantity χ is small when the separation between two particles, say 1 and 2, is much smaller than their separation with the third one: $r_{12} \ll r_{13}, r_{23}$.

We consider in this work the statistical properties of the shape distribution. To this end, we study the probability distribution functions of the various quantities R, I_2, w, and χ characterizing the shape. The Gaussian distribution $P_G(\rho_1, \rho_2) = \mathcal{N}\exp[-(\rho_1^2 + \rho_2^2)]$ provides an interesting distribution of reference. It can be shown [22] that the distributions of χ and w are uniform (in two dimensions): $P_G(\chi) = 6/\pi$ and $P_G(w) = 1$. In particular, the corresponding mean values are $\langle\chi\rangle_G = \pi/12$, $\langle w\rangle_G = 1/2$, and $\langle I_2\rangle_G = (1/2)(1 - \pi/4)$.

B. Monte-Carlo model

In order to study theoretically the distortion of sets of three or four particles by a turbulent flow in the inertial range of scales, a stochastic model based on phenomenological considerations was proposed in Ref. [21]. At the heart of the

model is a simplified scale decomposition of the full turbulent velocity field, on the scale of the global size of the triangle measured by the radius of gyration R [26]. Namely, the velocity field is written as

$$\boldsymbol{v} \equiv \boldsymbol{v}_< + \boldsymbol{v}_\approx + \boldsymbol{v}_>, \qquad (2.7)$$

where $\boldsymbol{v}_<$ is the contribution due to the small wave numbers or large scales in the usual Fourier decomposition ($|k| \leq 1/2R$), $\boldsymbol{v}_>$ comes from the large wave numbers ($|k| \geq 2/R$) or small scales, and $\boldsymbol{v}_\approx$ originates from the scales of the flow comparable to the global scale R ($2/R \leq |k| \leq 1/2R$). The large scale contribution is uniform over the triangular configuration of particles, and is therefore assumed in Ref. [21] not to distort the set of particles. The $\boldsymbol{v}_\approx$ part of the velocity field acts coherently over the scale of the triangles with correlation time of the order of the characteristic time of turbulence at scale R, defined by

$$\tau(R) = R^{2/3} \epsilon^{-1/3}. \qquad (2.8)$$

The small scale component $\boldsymbol{v}_>$ is often assumed to be completely incoherent on the scale R of the three points and its correlation time is short compared to the characteristic time of turbulence at scale $\tau(R)$. It is modeled in Ref. [21] by a white noise term.

The action of $\boldsymbol{v}_\approx$ is approximated by a (coarse-grained) strain matrix, $M_{ab} = \partial_a v_b$, acting on the vectors $\boldsymbol{\rho}_i$. The rapidly fluctuating incoherent component $\boldsymbol{v}_>$ is modeled by a Gaussian, white in time, random process. This leads to the following stochastic model [21]:

$$\frac{d\rho_i^a}{dt} = \rho_i^b M_{ab} + u_i^a, \qquad (2.9)$$

$$\frac{dM_{ab}}{dt} = -\frac{M_{ab}}{\tau(R)} + \eta_{ab}, \qquad (2.10)$$

where the indices $i,j = 1,2$ for three particles are labels of the relative vectors, see Eq. (2.2), and a,b labels of the spatial components. The velocity fields $\boldsymbol{u}$ and the η_{ab} term are random Gaussian terms, δ correlated in time with variances

$$\langle \eta_{ab}(t) \eta_{cd}(t') \rangle = C_\eta^2 \delta(t-t')(\delta_{ac}\delta_{bd} - \tfrac{1}{2}\delta_{ab}\delta_{cd})/\tau(R), \qquad (2.11)$$

$$\langle u_i^a(t) u_j^b(t') \rangle = \left(\frac{C_v}{2}\right)^2 \delta(t-t')\delta_{ij}\delta_{ab}R^2/\tau(R). \qquad (2.12)$$

The stochastic model has been constructed in such a way that the matrix M is traceless (incompressibility) and correlated with a time scale $\tau(R)$. Its amplitude is of the order of $|M| \sim R^{-1/3}$. The dimensionless parameter C_v (respectively, C_η) controls the importance of the incoherent jitter (respectively, of the coherent term) in the model.

Physically, the term $\rho_i^b M_{ab}$ in Eq. (2.10) stretches and aligns the set of points. This distorting action is opposed by the action of the $\boldsymbol{u}$ term, which tends to make the shape distribution Gaussian. The shape distribution resulting from

these two effects is nontrivial, and depends continuously on the ratio C_v/C_η. *A priori*, this number is of order 1. In the limit $C_v/C_\eta \to \infty$, the shape distribution becomes Gaussian.

The model turns out to reproduce qualitatively several important aspects of the experimental results. A detailed analysis of the experimental data, however, pointed out several shortcomings of the stochastic approach [22]. In particular, it was found that whereas the stochastic model predicts a uniform distribution of the variable χ, the experimental distribution of χ shows a peak near $\chi = 0$.

III. KINEMATIC SIMULATIONS

In contrast to the stochastic model described above, KS defines explicitly the velocity field that advects the particles. Following Ref. [27], we define the turbulent velocity field $\boldsymbol{v}(\boldsymbol{x},t)$ by summing over a set of Fourier modes, $\boldsymbol{k}_n$:

$$\boldsymbol{v}(\boldsymbol{x},t) = \sum_{n=1}^{N_k} [\boldsymbol{A}_n \times \boldsymbol{k}_n \cos(\boldsymbol{k}_n \cdot \boldsymbol{x} + \omega_n t)$$
$$+ \boldsymbol{B}_n \times \boldsymbol{k}_n \sin(\boldsymbol{k}_n \cdot \boldsymbol{x} + \omega_n t)], \qquad (3.1)$$

where N_k is the number of modes in the simulations, $\boldsymbol{k}_n$ are the wave vectors, $\boldsymbol{A}_n$ and $\boldsymbol{B}_n$ are the amplitude vectors and ω_n is the frequency. The norms of the wave vector are chosen of the form $k_n = |\boldsymbol{k}_n| = k_0 b^n$ with a parameter b typically chosen to be $b = (L/\eta)^{1/(N_k-1)}$. The large (integral) scale L and the small (Kolmogorov) scale η of the flow verify $L = 1/k_1$ and $\eta = 1/k_{N_k}$ ($L/\eta = b^{N_k}$). The direction of the wave vector, $\hat{k}_n = \boldsymbol{k}_n/|\boldsymbol{k}_n|$, is uniformly distributed along the unit circle. Similarly, the directions of the vectors $\boldsymbol{A}_n$ and $\boldsymbol{B}_n$ are randomly distributed, and their amplitudes are chosen so that the energy spectrum is of the form $E(k) \sim k^{-p}$. The frequencies ω_n are taken to be $\omega_n = \lambda \sqrt{k_n^3 E(k_n)}$, where λ is a dimensionless parameter, *a priori* of $\mathcal{O}(1)$. The definition, Eq. (3.1), makes the velocity field explicitly incompressible. Note that no δ correlation in time is used in KS at any level and that the parameter λ controls the unsteadiness of the flow.

To investigate the geometry of clusters of $n=3$ Lagrangian particles, we simply advect numerically Lagrangian particles in the velocity field $\boldsymbol{v}(\boldsymbol{x},t)$ defined by Eq. (3.1). This is done by solving a set of ordinary differential equations for the position vectors $\boldsymbol{x}(\boldsymbol{x}_0,t)$:

$$\frac{d}{dt}\boldsymbol{X}(\boldsymbol{x}_0,t) = \boldsymbol{v}(\boldsymbol{x}=\boldsymbol{X},t) \qquad (3.2)$$

with the initial condition $\boldsymbol{X}(\boldsymbol{x}_0,0) = \boldsymbol{x}_0$. We start with an isotropic object, i.e., with an equilateral triangle, of a given size, and follow its evolution over time. The quantities characterizing the deformation of the object, such as I_2, w, χ, are monitored as a function of time. We then perform ensemble averages over many triangles in different realizations of the velocity field to obtain the relevant particle statistics. We also checked that our results are not sensitive to the choice of

distribution and/or number of modes N_k used in the simulation, in general agreement with the corresponding tests in Ref. [25].

We first validate the predictions from KS with the experimental results [22]. To this end, we choose the power of the spectrum $p = 5/3$, the ratio of inner to outer scales as suggested by the experiment, and we take $\lambda = \mathcal{O}(1)$. We then extrapolate our results to higher values of the ratio of inner to outer scales L/η, to study dispersion in a high Reynolds number flow.

We stress that KS is a model of the Eulerian velocity field, used to advect the particles. The KS velocity field (3.1) has an interesting spatiotemporal flow structure, which varies with the parameters of the flow p and λ [26,27]. Investigating systematically how the changes in the parameters p and λ affects advection of particles is intrinsically interesting in the context of this study.

IV. VALIDATION OF KS

Before making any predictions with KS regarding multiparticle statistics we first validate the model by comparing with the experimental results Ref. [22]. We are interested here in reproducing *qualitatively* the experimental results of [22]. This does not mean that KS is not able to reproduce quantitative predictions, at the cost of fitting the parameter λ. We are merely interested in the trends of the shape evolution, that is, in the behaviors of the distributions of w, χ, etc., as a function of time.

An experimental investigation of the problem of dispersion of triangles by a turbulent flow was carried out in two dimensions, in the inverse cascade regime [22]. The flow was confined in a small container, 15×15 cm^2. Permanent magnets were placed under the bottom of the cell. The flow was stirred by running a current through a salted solution. The energy was injected at the scale $l_i = 1.5$ cm. The velocity field was recorded by using standard Particle Image Velocimetry techniques and was then stored on a 64×64 grid every 0.04 s. The resulting spatial resolution was good enough to describe all the relevant scales of the flow. A Kolmogorov $k^{-5/3}$ regime was observed over the limited range of scales 1.5 cm $\leq l \leq 5.5$ cm. The time resolution was also amply sufficient to follow numerically the evolution of particles. The evolution of a large number ($\sim 2 \times 10^4$) of triangles was then followed numerically. In this section we compare our results produced from KS with the experimental results of Ref. [22] and validate our model in the process.

It was observed (see Figs. 3–5 of Ref. [22]) that the typical size measured by the radius of gyration R of the triangles increased until it reached the largest scale 9 cm of the experimental setup where it started to fluctuate around this value. The evolution in time of the mean values of w and χ (see Figs. 4 and 5 of Ref. [22]) showed a rapid decrease of these parameters corresponding to strong shape distortions of the triangles. The smaller the initial separation r_0, the lower the minimal value of this parameter was observed. The shape distortion was maximum when R reached the lower value $\sqrt{R^2} = 1.5$ cm of the inertial range. The mean values of these variables tend to an asymptotic value when R increases
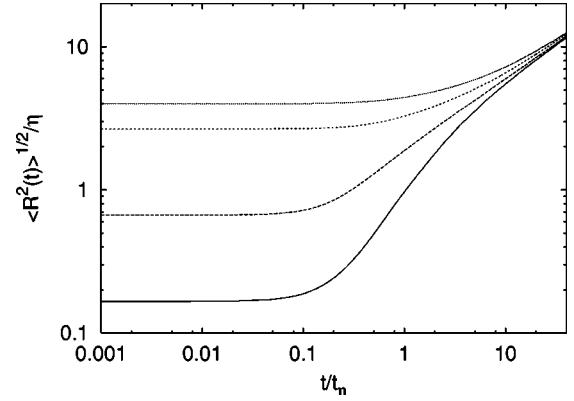

FIG. 1. Time evolution of $\langle R^2 \rangle$ for different values of r_0.

above the upper bound $\sqrt{R^2} = 5.5$ cm of the inertial range. Specifically, it was found that $\langle w \rangle_{asm} = 0.5$, $\langle I_2 \rangle_{asm} \approx 0.11$, and $\langle \chi \rangle_{asm} \approx 0.26$. These asymptotic values for w, I_2, and χ correspond to a Gaussian distribution of $\boldsymbol{\rho}_1$ and $\boldsymbol{\rho}_2$, which implies a uniform distribution for w, I_2, and χ with the Gaussian values $\langle w \rangle_{Gau} = 1/2$, $\langle I_2 \rangle_{Gau} = (1 - \pi/4)/2 = 0.107$, and $\langle \chi \rangle_{Gau} = \pi/12 = 0.262$ and a corresponding Gaussian distribution for R: $P_{Gau}(R) = (8R^3/\langle R^2 \rangle^2) \exp(-2R^2/\langle R^2 \rangle)$.

The probability distribution function (PDF) of R and w, see Fig. 6 of Ref. [22], can be well approximated by the Gaussian distribution for large values of time $t = 80$ s and $t = 100$ s, corresponding to the values of the radius of gyration larger than the integral scale L. At later times, the finite size of the experimental system induces a saturation of the triangle size, so the tails of the distribution of R could no longer be correctly fitted by $P_{Gau}(R)$ [22]. A very slow relaxation of the value of $\langle \chi \rangle$ towards its asymptotic, Gaussian value was observed. The fact that $\chi = 0$ is more probable than $\chi = \pi/6$ implies that triangles with one edge much shorter than the two other ones has a large probability. This effect should ultimately disappear at later time, in the diffusive regime.

The numerical experiment, consists of generating KS flows in two dimensions, with an energy spectrum $E(k) \sim k^{-5/3}$, similar to that observed experimentally, characterized by a ratio $L/\eta = 3.67$, and with an unsteadiness factor $\lambda = 0.5$. The smallest and the largest time scales of the flow are defined to be $t_\eta = 2\pi/\sqrt{k_\eta^3 E(k_\eta)}$ and $t_E = L/u'$, respectively, where u' is the rms velocity of the flow field. In this flow, we follow the evolution of three points, initialized as the vertices of an equilateral triangle of size r_0. The results were averaged over $\sim 10^4$ configurations.

The results obtained from KS show the same tendencies as that observed in the experiment, as we now demonstrate. All the figures in this paper have been plotted against dimensionless quantities.

The behaviors as functions of time of the mean values of $\langle R \rangle$ (see Fig. 1), $\langle w \rangle$ (see Fig. 2) and $\langle \chi \rangle$ (see Fig. 3), as well as the evolution of the PDFs of R, w and χ (see Fig. 4) computed from KS are very close to those observed experimentally (see Figs. 3–6 of Ref. [22]). Contrary to the labo-
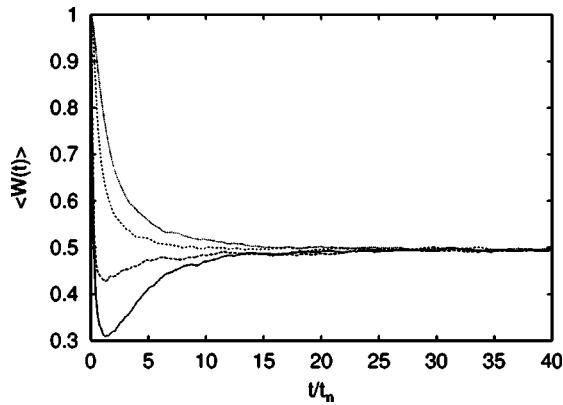
FIG. 2. Time evolution of $\langle w \rangle$ for different values of r_0.

ratory experiment, where the spatial confinement of the setup induced a saturation of the growth of the radius of gyration, $\langle R^2 \rangle$ grows like t at very long times. The distribution of sizes, R, as well as the distribution of w and χ are Gaussian in this regime. The relaxation of the peak of probability for $\chi \approx 0$ is faster in the KS than in the experiment. This small discrepancy is conceivably due to the large scale limitations of the flow.

At intermediate time scales, when $\langle R^2 \rangle^{1/2}$ is in the inertial range, the mean values and the distribution of w are very close to those observed in Ref. [22].

These results demonstrate that KS reproduces very well the main properties of the evolution of three Lagrangian particles. A similar conclusion was reached in Ref. [24] by comparing laboratory and KS results in two dimensions, and in Ref. [25] by comparing DNS and KS results in three dimensions. KS is thus a potentially very useful tool both for fundamental studies, and for dispersion studies in a more applied context.

V. PREDICTIONS OF KS IN THE LARGE REYNOLDS NUMBER LIMIT

The results of the preceding subsection demonstrate that the KS model reproduces quite satisfactorily the laboratory results concerning the evolution of three particles in a turbulent two-dimensional flow. We now investigate the large Reynolds number limit with the help of the KS. This is
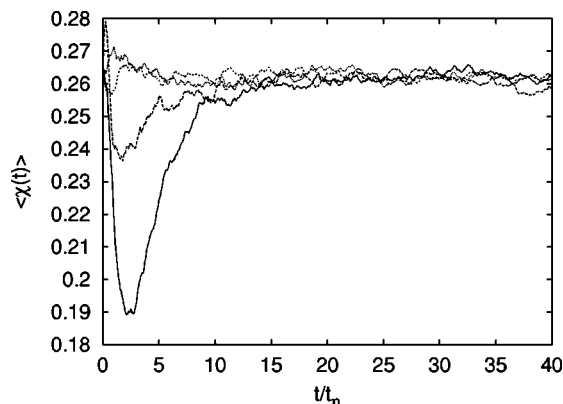

FIG. 3. Time evolution of $\langle \chi \rangle$ for different values of r_0.

achieved by increasing the ratio of the largest to the smallest scale, L/η irrespective of initial conditions.

A previous study [24] has shown that the separation between two particles in the inertial regime shows sizable differences compared to the famous Richardson's scaling, according to which the separation grows according to $\langle R^2 \rangle \propto \epsilon t^3$ irrespective of initial conditions. Specifically a strong dependence of two-particle dispersion statistics on the initial separation the particles was found [24]. In the case of three particles studied here, it is of obvious interest to investigate the statistics of the radius of gyration of the set of particles. Also, the existence of a nontrivial, time-independent distribution of shapes, predicted by Ref. [21], when the separation between particles is in the inertial range of scales, remains to be tested. We address these questions, in turn, with the help of KS.

We stress that there is no guarantee that the evolution of three particles is correctly predicted by the KS with $p = 5/3$ when the ratio L/η becomes large. In spite of this uncertainty, the numerical results presented here are intrinsically interesting since the KS flow shares with real turbulence a number of important properties.

The evolution of three particles has been followed numerically, using several KS flows, corresponding to different Reynolds numbers, or equivalently, to different values of L/η ($L/\eta = 1691, 3381, 16909$). Our runs, with the values of the parameters characterizing the flows, are listed in Table I. We note in passing that the Reynolds number Re and the Taylor-based Reynolds number Re_λ are related to L/η by $Re \sim (L/\eta)^{4/3}$ and $Re_\lambda \sim (L/\eta)^{2/3}$.

The results of these simulations (Fig. 5, corresponding to $L/\eta = 1691$ and Fig. 6, corresponding to $L/\eta = 16909$) show some resemblance with the small L/η case (see Sec. IV). As the Reynolds number is increased, the dependence of the variables describing geometry, $\langle I_2 \rangle$, $\langle W \rangle$, and $\langle \chi \rangle$ becomes weaker, both as a function of the initial size of the triangle and as a function of time. The values of these variables is always significantly different from the Gaussian values.

The PDFs of R, w, and χ at the value $L/\eta = 1691$ also show trends that are similar to those observed at smaller values of L/η (Fig. 7). We have not followed particles long enough to see the Gaussian distribution of shapes at very large values of L/η; the study has been restricted to the nontrivial inertial range. In this range of scales, the variation of the PDF as a function of time is considerably weaker than observed in Sec. IV, and in this sense, the results suggest that one may be getting close to the self-similar shape distribution predicted in Ref. [21]. A visible deformation of the PDF of R can be observed as a function of time, reflecting the fact that at the later times large excursions in the radius of gyration are getting close to the value of the largest available scale L.

Although still finite, the value of L/η for run 13 is significantly larger than it is in any engineering, industrial, or laboratory flow. Even so, our numerical results show persistent differences with the picture of a simple truly self similar regime.

In all the reported DNS, in two [29] and in three dimensions [30], a dependence of the behavior of $\langle R(t) \rangle$ on the
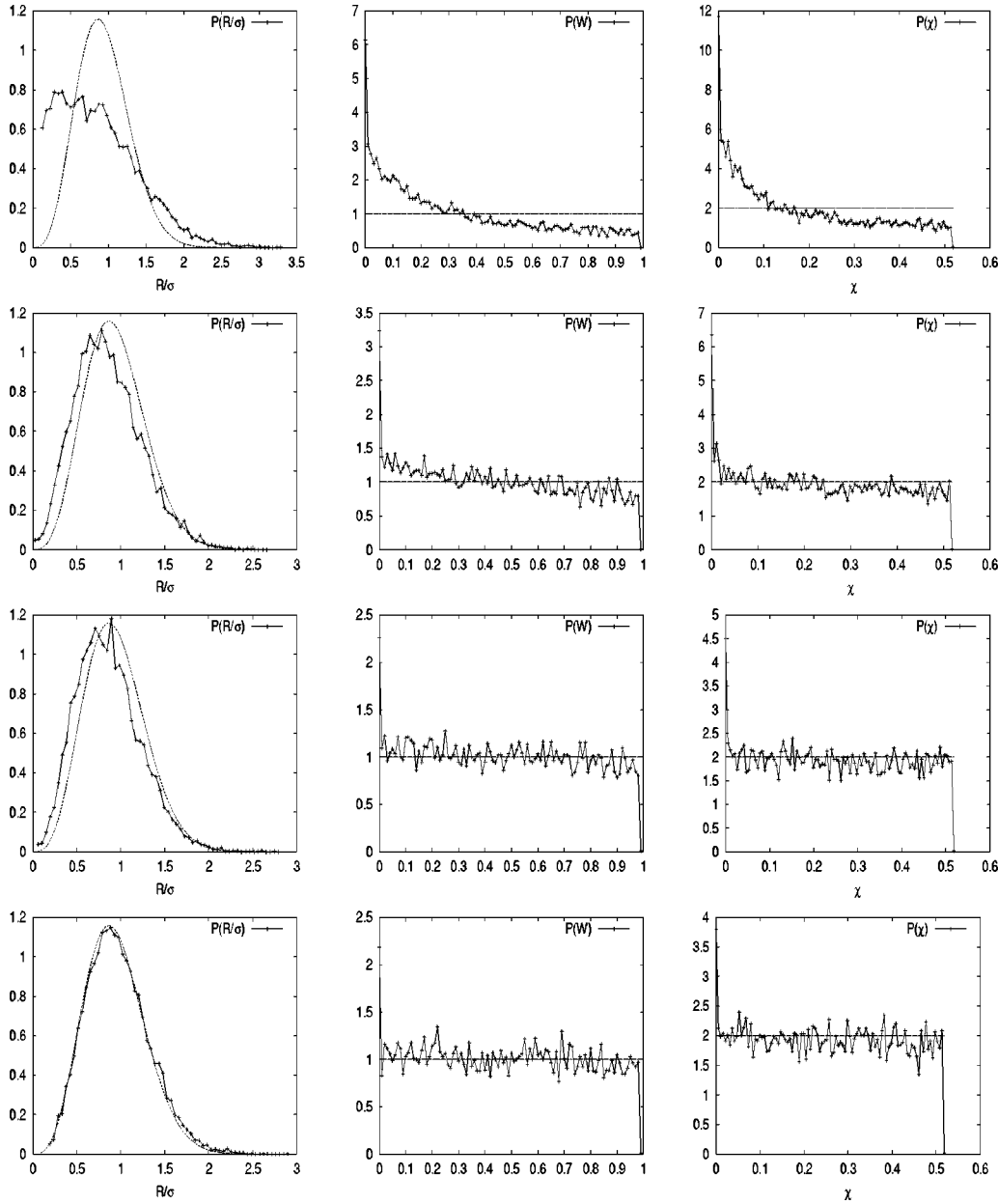
FIG. 4. Time evolution of the PDFs of R/σ ($\sigma = \sqrt{\langle R^2 \rangle}$), w, and $\chi(rad)$ for $r_0/\eta = 1/6$ in 2D KS, with $L/\eta = 3.67$, $t_E/t_\eta = 2.3$, and $\lambda = 0.5$. From top to bottom the figures are shown at times $t = 2 \times t_\eta$, $t = 6 \times t_\eta$, $t = 10 \times t_\eta$, and $t = 14 \times t_\eta$, respectively. The light lines correspond to the Gaussian predictions $P(R) = 8(R/\sigma)^3 \exp[-2(R/\sigma)^2]$, $P(w) = 1$, and $P(\chi) = 6/\pi$ [22].

initial separation r_0 has been reported. We observe a similar behavior in our KS calculation. Figure 8 shows that the t^3 Richardson regime is never really reached. Instead, a continuous dependence of the variation of $\langle R^2 \rangle/t^3$ on the initial separation r_0 is observed. This effect is clearly seen, even at our largest Reynolds number. This behavior suggests that the set of three particles always remembers its initial condition, which represents a departure with respect to the Richardson prediction. Also, at a fixed value of the initial size of the triangle, a nontrivial power seems to emerge as the Reynolds number increases. A similar behavior was observed for the separation between two particles [24].

To investigate further this effect, we consider the PDFs of the radius of gyration, R. Figure 9 shows a superposition of

the PDFs of $R/\langle R \rangle$ for three different initial values of $r_0/\eta = 0.1, 1.0, 5.0$, and at different values of time. The distribution of the large values of $R/\langle R \rangle$ are expected to be independent of time and Fig. 9 does not disprove this expectation. However, the distribution at small values of $R/\langle R \rangle$ seems to vary throughout the entire evolution.

To compare different values of r_0, we have plotted the PDFs of $R/\langle R \rangle$ corresponding to two different values of r_0, but with similar values of $\langle R \rangle$ (Figs. 10 and 11). For large enough times the PDFs of $R/\langle R \rangle$ seem to collapse at large values of $R/\langle R \rangle$ within statistical errors. However, serious deviations are observed at small values of $R/\langle R \rangle$. In particular, the peaks of the PDF at very small values of $R/\langle R \rangle$ are much sharper at smaller values than at larger values of r_0.

TABLE I. Different simulation parameters of our runs with kinematic simulation.

No. of Runs	L/η	No. of Triangles	r_0/η	λ	No. of Modes N_k	$E(k) \sim k^{-p}$ p
1	3.67	1×10^4	1/6,2/3,8/3,4	0.5	79	1.67
2	10	1×10^4	0.05,0.5,5	0.5	79	1.67
3	1691	1×10^4	0.5,5,20,64	0.5	79	1.67
4	1691	1×10^4	0.5	1.5	79	1.67
5	1691	1×10^4	0.5	5.0	79	1.67
6	1691	1×10^4	0.5	10.0	79	1.67
7	1691	1×10^4	0.5	0.5	79	1.20
8	1691	1×10^4	0.5	0.5	79	1.33
9	1691	1×10^4	0.5	0.5	79	1.40
10	1691	1×10^4	0.5	0.5	79	1.80
11	3380	5×10^4	5,20,64	0.5	200	1.67
12	11180	1×10^4	5,64	0.5	500	1.67
13	16909	1×10^4	5,20,64	0.5	500	1.67

These results suggest that the distributions of R are influenced throughout the entire evolution by the initial value r_0, insofar as a significant number of triplets do not really separate, and remain at a value $R \sim r_0$. In the case of two particles this behavior has indeed been observed by Jullien *et al.* [18] in the laboratory for low Reynolds number flows and by Fung *et al.* [27] and Nicolleau *et al.* [24] in high Reynolds number KS simulations. In this way, the evolution depends in an essential way on the value of r_0.

The evolution of other geometric quantities, such as $\langle w \rangle$, $\langle \chi \rangle$, reflects to some extent the behavior described above (see Figs. 5, 6). Indeed, the lack of exact self-similarity observed in the evolution of the radius of gyration, R, shows that the prediction of a truly time independent shape distribution is at best valid at Reynolds numbers impossible to attain. Although this prediction might constitute a good first-order approximation, which becomes better as the Reynolds number increases, Fig. 6 shows that the mean values of w, I_2, and χ *do* vary with time, even at $L/\eta = 16909$. In addition, a systematic variation with r_0 is seen in Figs. 5 and 6. The distributions are observed to remain non-Gaussian as long as $\langle R \rangle$ remains in the inertial range, and do correspond to a higher probability of observing elongated objects, as anticipated in the stochastic model proposed in Refs. [19,21]. In the light of the KS results, the stochastic model correctly predicts the main qualitative feature (the increased probability of elongated objects), but it does not incorporate the lack of self-similarity of multiparticle diffusion observed in KS. As we discuss in the following paragraph, memory effects relating to this lack of self-similarity are observed in laboratory experiments [18,22]. They are also observed in KS because, unlike stochastic models, KS incorporates the persistence of flow structures. Whether this lack of self-similarity persists in the laboratory and in nature at extremely high Reynolds numbers remains an open question.

The results obtained so far suggest that the lack of self-similarity in the evolution of the radius of gyration, R, is due to the fact that particles stay together, at a distance of order r_0 with a high probability. Even if the radius of gyration grows to a value $R \gg r_0$, it was observed in Ref. [22] that two particles of the triplet can remain close to each other, with a large probability. We interpret the lack of a stationary distribution of shapes to reflect a similar cause: when one particle of the triplet separates from the two other ones, which remain at a mutual distance $\sim r_0$, a very elongated shape is created. The relaxation of the distribution of shapes towards a stationary distribution will depend on how the two particles that are close together eventually separate. Our observations suggest that, the smaller the r_0, the longer the particles will stay together, and hence, the longer it will take the transient to relax. This lack of self-similarity is absent in stochastic models, such as those proposed by Ref. [19], and is consistent with the view that coherent streamline structures are persistent enough to cause a dependence of turbulent diffusion on initial conditions.

VI. EFFECTS OF PERSISTENCE OF THE FLOW STRUCTURE

The KS model allows us to modify some of the characteristics of the advecting flow, both spatially and temporally. This is achieved by modifying the parameters λ and p. The purpose of this section is to investigate the effect of changing the spatiotemporal structure of the flow, and in this way, to gain insight into the mechanisms involved in multiparticle dispersion.

We first change the temporal structure of the flow by varying the persistence parameter λ (see Fig. 12). This controls how fast the streamlines of the flow are jittered in comparison to the relevant eddy turn over time at the corresponding scale. This jittering makes the particles in the flow to be rapidly swept from one streamline to the other. Since in KS there is no interaction among modes of the velocity field, this jittering mimics the sweeping effects that are present in a real flow field. The minima of $\langle I_2(t) \rangle$ and $\langle w(t) \rangle$ increase with increasing unsteadiness parameter λ within the inertial range
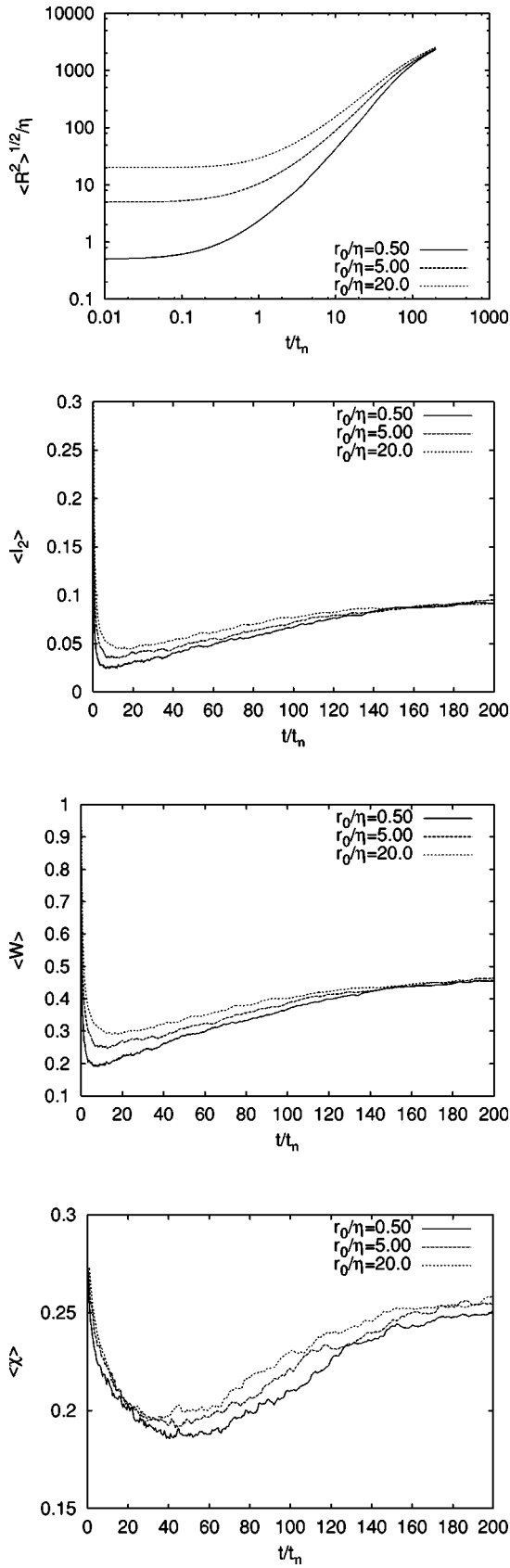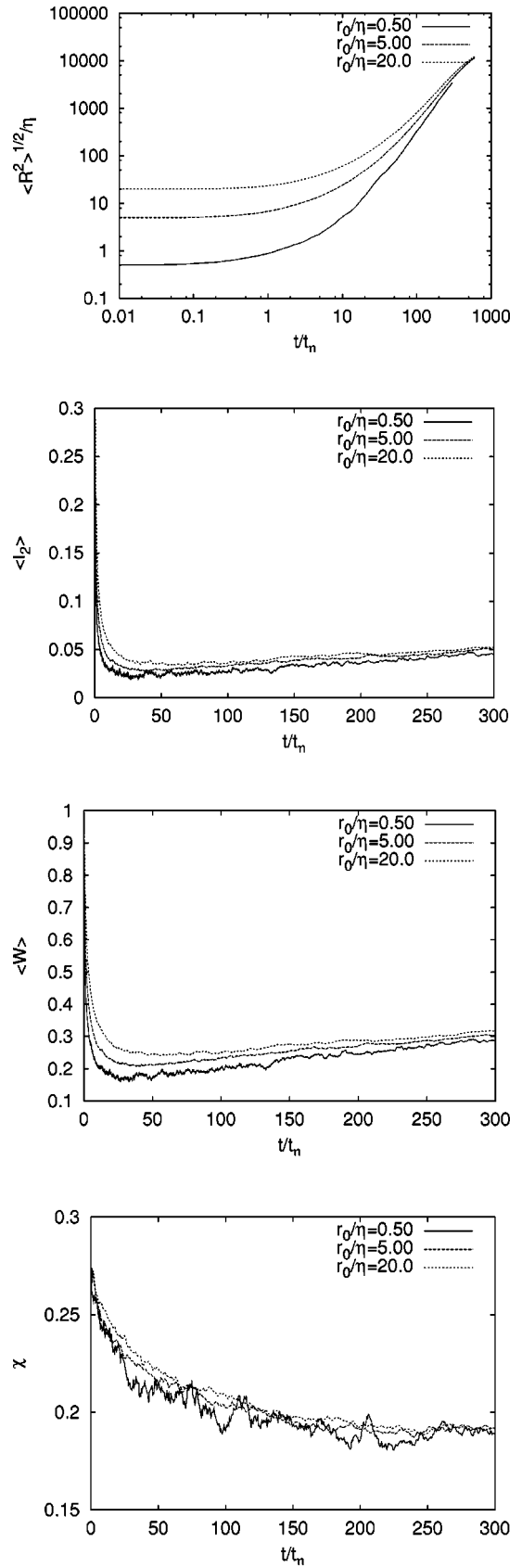
FIG. 5. Time evolution of $\langle R(t) \rangle$, $\langle I_2(t) \rangle$, $\langle w(t) \rangle$, and $\langle \chi(t) \rangle$ produced by kinematic simulation (KS) in 2D for $L/\eta = 1691$ and $\lambda = 0.5$ with $t_E/t_\eta = 82.1$.

FIG. 6. Time evolution of $\langle R(t) \rangle$, $\langle I_2(t) \rangle$, $\langle w(t) \rangle$, and $\langle \chi(t) \rangle$ produced by KS in 2D for $L/\eta = 16909$ and $\lambda = 0.5$ with $t_E/t_\eta = 538.1$.
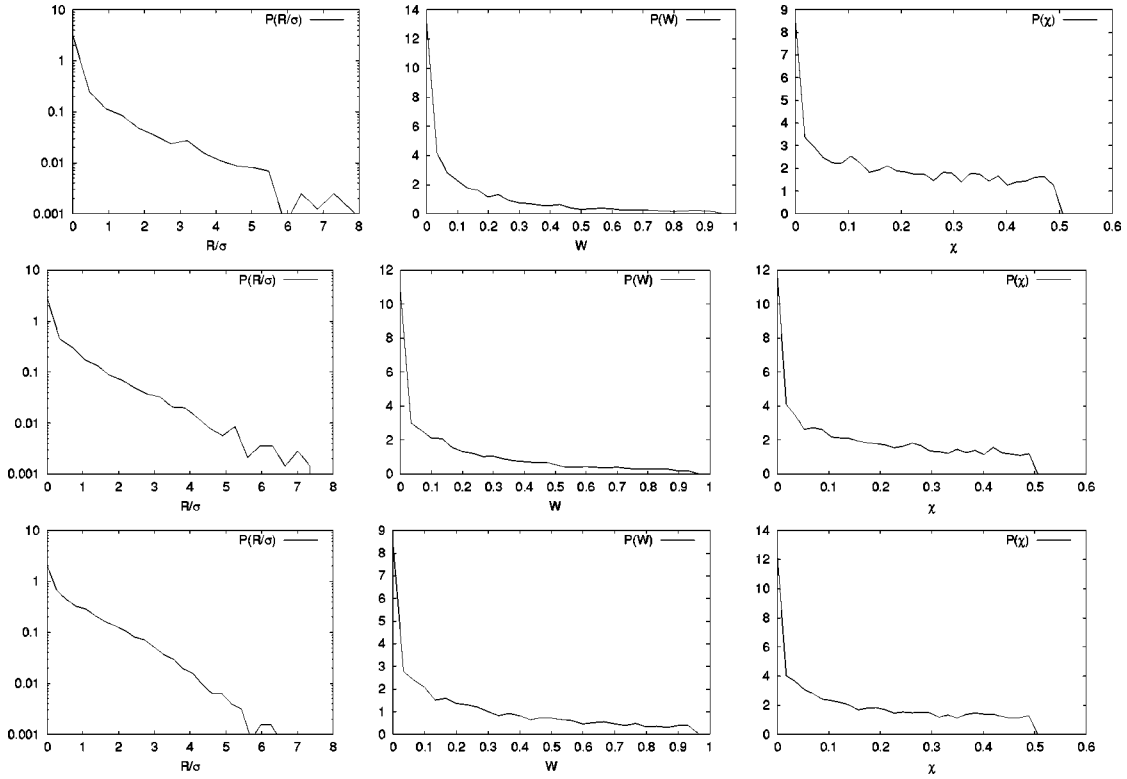
FIG. 7. Time evolution of the PDFs of R/σ, w, and $\chi(rad)$ for $r_0/\eta = 0.5$ in 2D KS, with $L/\eta = 1691$ and $\lambda = 0.5$ with $t_E/t_\eta = 82.1$. From top to bottom the figures are shown at times $t = 20 \times t_\eta$, $t = 60 \times t_\eta$, and $t = 100 \times t_\eta$, respectively.

of time scales, which means triangles are less elongated for larger values of λ (Fig. 12). This happens because the paths of the neighboring particles decorrelate faster for larger values of λ and triangles quickly forget their memory of the initial state. Hence increased values of λ should cause the triangle shape parameters to relax faster to their corresponding Gaussian values.

Second, we change the spatial structure of the flow field by changing the energy spectrum, i.e., changing the exponent p in $E(k) \sim k^{-p}$ (see Fig. 13). This has the effect of changing the density of straining regions in the flow field [27,28], thereby modifying the separation mechanism of particle pairs and clusters. The minimum of $\langle I_2(t) \rangle$ and $\langle w(t) \rangle$ decreases with increasing p ($E(k) \sim k^{-p}$) within the inertial range of time and scales. This means that the clusters are more (less) elongated during the inertial range of times when p is made larger (smaller). An explanation of this effect can be given in terms of randomness: as p increases, there is less energy in the smaller scales of the turbulence, which may mean less randomness leading to clusters remaining more elongated during the inertial range of times. In the context of KS, as p increases, there is indeed less energy in the small scales leading to smaller unsteadiness frequency $\omega_n \sim k_n^{(3-p)/2}$ and therefore less randomness and more elongated clusters. However, a more searching explanation should invoke the spatio-temporal flow mechanism causing cluster elongation. One such mechanism already proposed in the literature [23,27] is based on persistent effects of straining regions. The spatial density of straining regions decreases as p is made larger [27,28].

However, the simple calculation, presented in the Appendix, indicates that the average straining rate per straining region increases faster than the number of such regions decreases when p is made larger. Provided that the effect of increased strain rate per strain region overwhelms that of the decreased number of such regions, then the same conclusion is reached: clusters should remain more (less) elongated during the inertial range of times when p is made larger (smaller).

VII. CONCLUSIONS

We have investigated the Lagrangian shape dynamics and the corresponding statistics of multiple particles, namely, of three particles advected by a two-dimensional turbulent flow. We have used KS to generate a turbulent velocity field and follow numerically sets of three particles in this flow field. The results of the simulation have been compared with the results of a two-dimensional experiment [22]. We have identified a mechanism for the shape evolution of three particles depending on the underlying flow structure and the effect of persistence of these structures on the statistics of these shapes.

Two regimes with well-characterized distributions have been identified in our simulation with KS, as observed in the experiment of Castiglione *et al.* [22].

The first regime is characterized by the fact that the mean separation between particles is large compared to the largest scale of the flow (diffusion regime); the shape distribution is Gaussian.
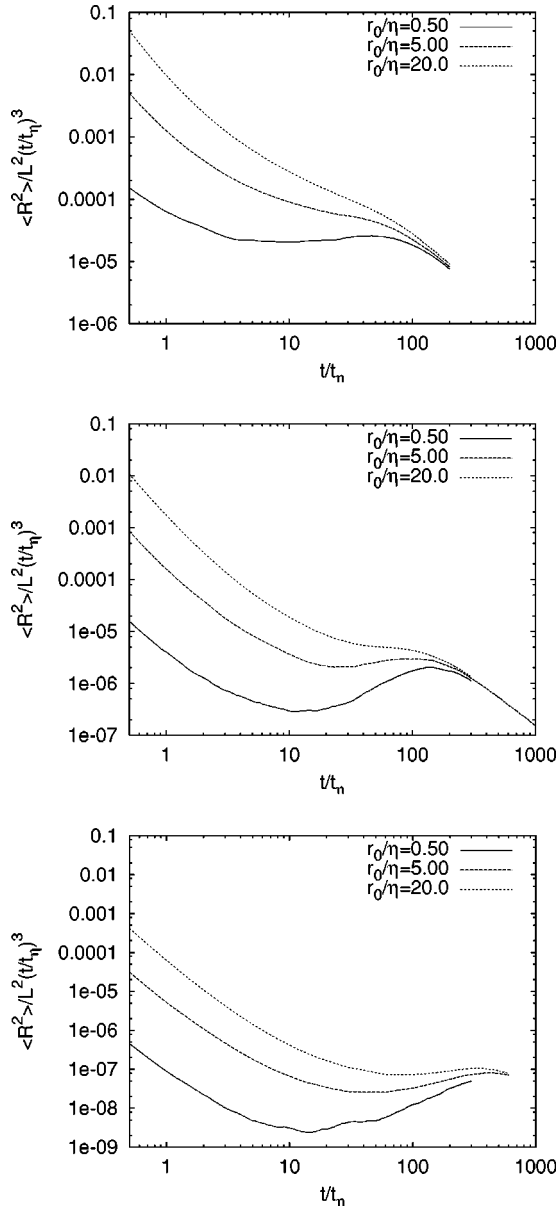
FIG. 8. Time evolution of $\langle R(t)^2 \rangle /(t/t_\eta)^3$ obtained by kinematic simulation of a triangular configuration of three particles in a two-dimensional high Reynolds number ($L/\eta = 1691, 3381$, and 16909) turbulent flow for different initial separation r_0's. Here the energy spectrum $E(k) \sim k^{-5/3}$, $\lambda = 0.5$, and the number of realizations is 5×10^3.
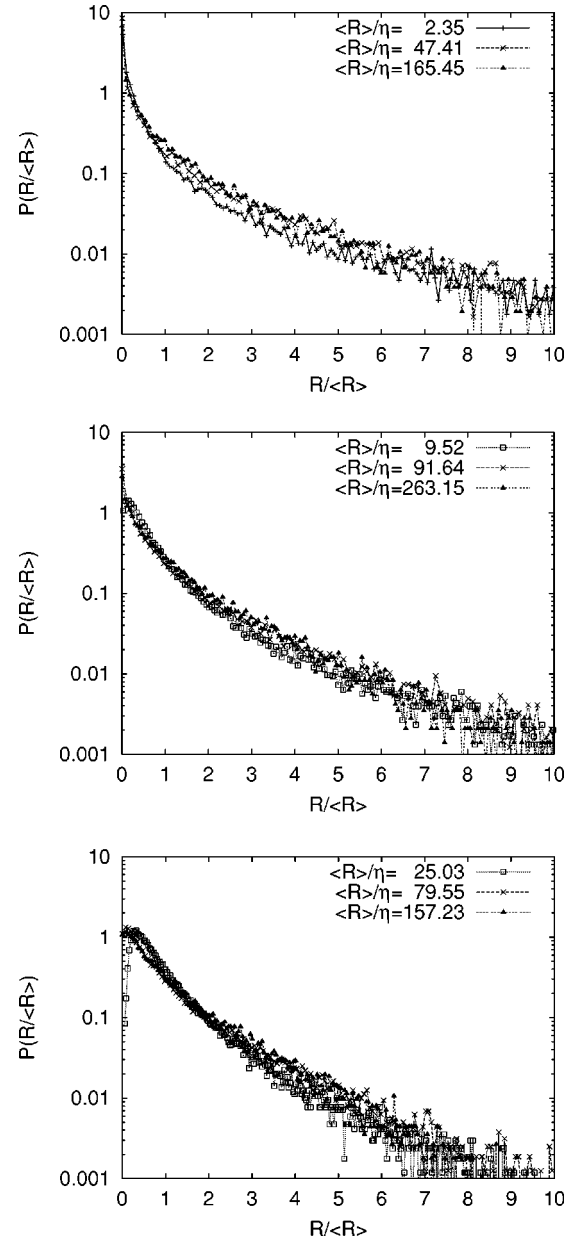

FIG. 9. Time evolution of the PDF of R with different r_0's obtained by KS in two dimensions with $E(k) \sim k^{-5/3}$, $L/\eta = 3381$. From left to right $r_0/\eta = 0.10, 1.0$ and 5.0.

The main result of this work concerns the other regime, where the mean separation between particles is in the inertial range: $\eta^2 \ll \langle R^2 \rangle \ll L^2$. We have found that in this regime, the shape distribution is nontrivial, as predicted phenomenologically in Ref. [21]. The temporal evolution of $\langle I_2(t) \rangle$, $\langle W(t) \rangle$, and $\langle \chi(t) \rangle$ match with the experimental results of Ref. [22]. KS also reproduces the correct distribution of these quantities. The stochastic model can do as well, except for the PDF of χ. In the inertial range of scales, the evidence for Richardson's law, $\langle R(t) \rangle \propto t^3$, remains elusive.

It is found that the clusters are more (less) elongated during the inertial range of times when λ is made smaller

(larger) (Fig. 12). The reason for this result must be that the persistence of the straining action of the flow is diminished when the flow is made more unsteady by increasing λ.

It is also found that the clusters are more (less) elongated during the inertial range of times when p is made larger (smaller). An explanation of this effect can be given in terms of randomness: as p increases, there is less energy in the smaller scales of the turbulence, which may mean less randomness leading to clusters remaining more elongated during the inertial range of times. However, we also discuss a more searching explanation that invokes the straining mechanisms causing cluster elongation.

The dependence of the shape of clusters on the initial separation between marked fluid elements is clearly demon-
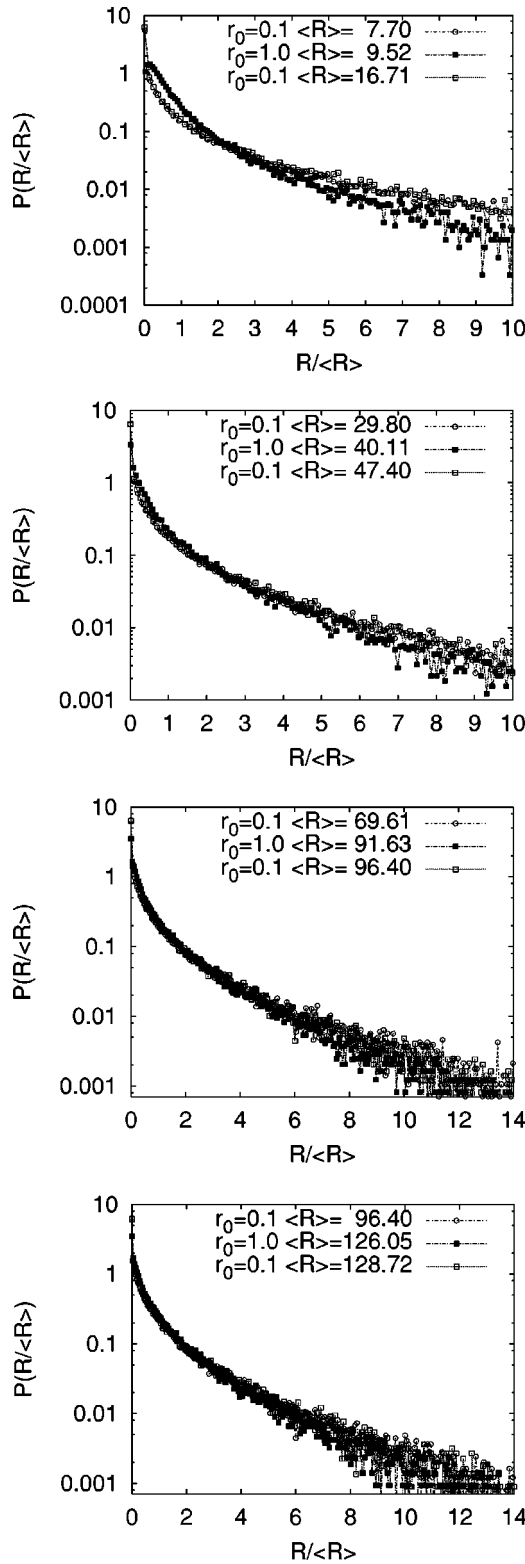
FIG. 10. PDF of radius of gyration, R, or global size with different values of r_0. Here both r_0 and $\langle R \rangle$ have been normalized by η. Two runs with different initial sizes are compared. The PDFs are shown at several times, for $r_0 = 0.1$ and $r_0 = 1.0$. For comparison, the PDFs of R corresponding to $r_0 = 0.1$ are shown at two times where the value of $\langle R(t) \rangle$ are the closest to the value of $\langle R(t) \rangle$ obtained with the larger value of r_0. The other parameters of the runs are $L/\eta = 3381$, $\lambda = 0.5$, and $t_E/t_\eta = 130.2$.
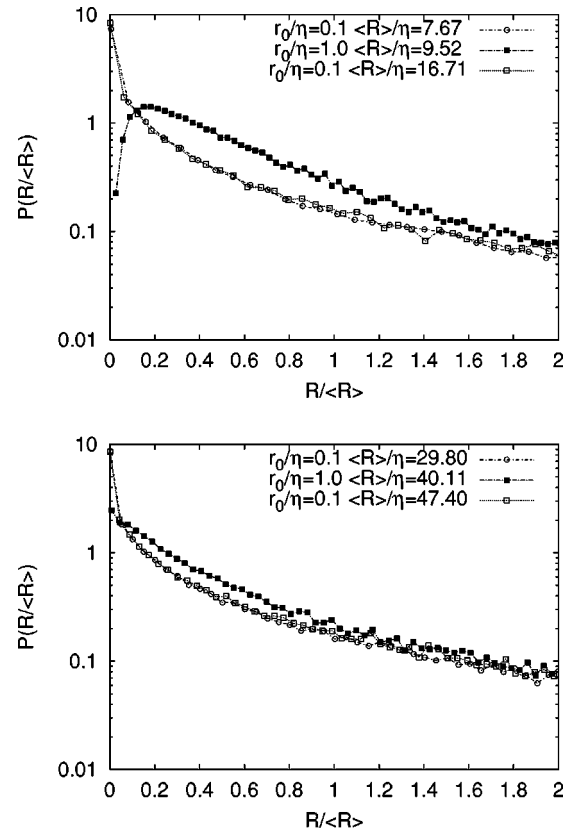
FIG. 11. PDF of radius of gyration, R, with two different values of the initial separation r_0: $r_0 = 0.1$ and 1.0. The plots in this figure are the zoomed versions of the corresponding plots in Fig. 10.

strated by the PDF of the radius of gyration of particle clusters with different initial separations not collapsing within the inertial range (see Figs. 10 and 11). Our KS numerical experiments indicate that clusters tend to have memory of the initial state even when the turbulence has an extremely wide inertial range of more than four decades.

This result is in agreement with the observed dependence [24] on the initial pair separation of the apparent power-law governing the growth of interparticle distances. If these effects are transient and due to a finite range of inertial scales, then our results indicate that they might only disappear at extremely high Reynolds numbers. However, the possibility should also be retained that these effects are not finite range transient effects, and are caused, instead, by the persistence of spatial flow structures at all scales, assuming this persistence remains at asymptotically high Reynolds numbers.

It is not clear how the results of this work apply to the problem of dispersion by a real velocity field. This study, however, demonstrates that the scale hierarchy of the flow leads to nontrivial shape statistics. A non-Gaussian shape distribution is thus very likely to be found in real flows when the inertial range is very large.
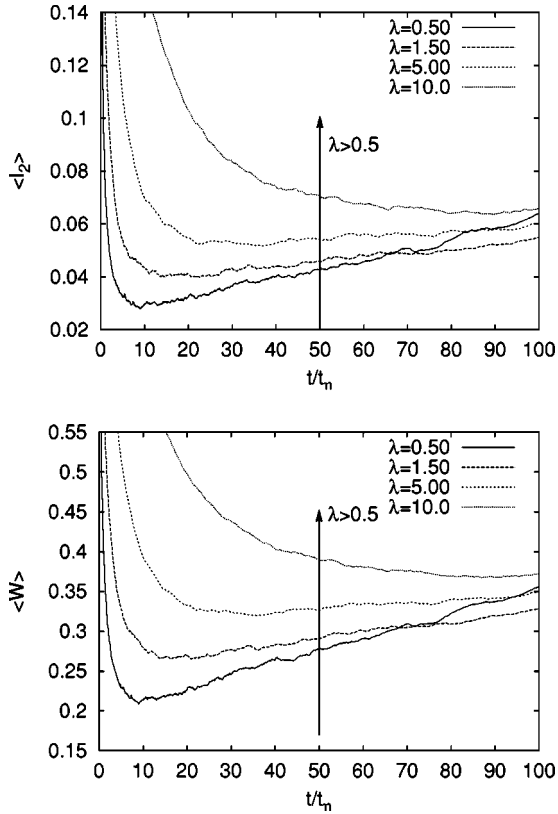
ACKNOWLEDGMENTS

FIG. 12. Time evolution of $\langle I_2(t) \rangle$ and $\langle w(t) \rangle$ obtained by kinematic simulation of a triangular configuration of three particles in a two-dimensional high Reynolds number ($L/\eta = 1691$) turbulent flow for different λ's. Here the energy spectrum $E(k) \sim k^{-5/3}$, initial separation $r_0 = 0.5\eta$, and number of realizations is 5×10^3.
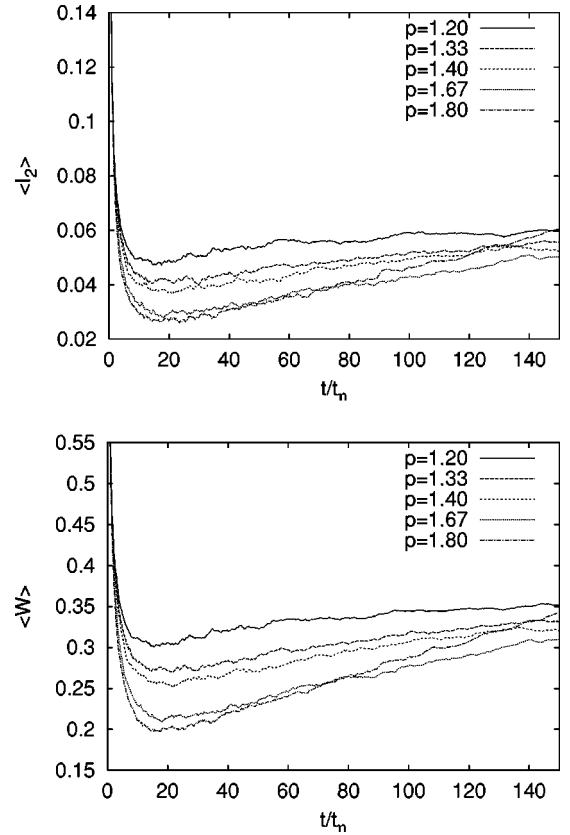

FIG. 13. Time evolution of $\langle I_2(t) \rangle$ and $\langle w(t) \rangle$ obtained by kinematic simulation of a triangular configuration of three particles in a two-dimensional high Reynolds number ($L/\eta = 1691$) turbulent flow for different energy spectra $E(k) \sim k^{-p}$. Here $\lambda = 0.5$, initial separation $r_0 = 0.5\eta$, and number of realizations is 5×10^3.

APPENDIX

Assume that we are given the spectrum $E(k) = E_0 L (kL)^{-p}$ defined in the range $1/L \leqslant k \leqslant 1/\eta$ of an isotropic turbulence. The mean square straining rate $\langle (\partial u/\partial x)^2 \rangle$ is proportional to $\int_{1/L}^{1/\eta} k^2 E(k) dk$. Substituting the form of the spectrum and integrating we get for $p < 3$,

$$\left\langle \left(\frac{\partial u}{\partial x} \right)^2 \right\rangle \sim \frac{E_0}{(3-p)L^2} \left(\frac{L}{\eta} \right)^{3-p}. \tag{A1}$$

In KS, the number density of straining stagnation points decreases with increasing p [27] and Ref. [28] calculated the following scaling relation:

$$n_s \sim \left(\frac{L}{\eta} \right)^{D_s}, \tag{A2}$$

where n_s is the number density of straining stagnation points and D_s is the fractal dimension of the spatial distribution of these points in the flow. In 2D KS, $D_s = 3 - p$ [28]. Hence, the number of straining stagnation points per unit area decreases with increasing p in our KS, but the mean square strain rate per straining stagnation point, i.e., $\langle (\partial u/\partial x)^2 \rangle / n_s$, scales like $E_0/(3-p)L^2$. This implies that, although the number density decreases with increasing p, but the mean strain rate per straining stagnation point becomes stronger, which is the reason behind the decrease of the parameters $\langle I_2 \rangle$ and $\langle W \rangle$ with increasing p.

[1] B.I. Shraiman and E.D. Siggia, Nature (London) **405**, 639 (2000).
[2] P.K. Yeung, Annu. Rev. Fluid Mech. **34**, 115 (2002).
[3] B. Sawford, Annu. Rev. Fluid Mech. **33**, 289 (2001).
[4] S.B. Pope, Annu. Rev. Fluid Mech. **26**, 23 (1994).
[5] G.K. Batchelor, Proc. Cambridge Philos. Soc. **48**, 345 (1952).
[6] L.F. Richardson, Proc. R. Soc. London, Ser. A **110**, 709 (1926).
[7] C. Gibson, C. Freihe, and S. McConnell, Phys. Fluids **20**, S156 (1977).
[8] P.G. Mestayer, J. Fluid Mech. **125**, 475 (1982).

[9] K.R. Sreenivasan, Proc. R. Soc. London, Ser. A **434**, 165 (1991).

[10] L. Mydlarski and Z. Warhaft, J. Fluid Mech. **358**, 135 (1998).

[11] B.I. Shraiman and E.D. Siggia, Phys. Rev. E **57**, 2965 (1998).

[12] A. Pumir, Phys. Rev. E **57**, 2914 (1998).

[13] L. Mydlarski, A. Pumir, B.I. Shraiman, E.D. Siggia, and Z. Warhaft, Phys. Rev. Lett. **81**, 4373 (1998).

[14] G. Falkovich, K. Gawedzki, and M. Vergassola, Rev. Mod. Phys. **73**, 913 (2001).

[15] A. La Porta, G.A. Voth, A.M. Crawford, J. Alexander, and E. Bodenschatz, Nature (London) **409**, 1017 (2001).

[16] S. Ott and J. Mann, J. Fluid Mech. **422**, 207 (2000).

[17] N. Mordant *et al.*, Phys. Rev. Lett. **87**, 214501 (2001).

[18] M.C. Jullien, J. Paret, and P. Tabeling, Phys. Rev. Lett. **82**, 2872 (1999).

[19] M. Chertkov, A. Pumir, and B.I. Shraiman, Phys. Fluids **11**, 2394 (1999).

[20] A. Celani and M. Vergassola, Phys. Rev. Lett. **86**, 424 (2001).

[21] A. Pumir, B.I. Shraiman, and M. Chertkov, Phys. Rev. Lett. **85**, 5324 (2000).

[22] P. Castiglione and A. Pumir, Phys. Rev. E **64**, 056303 (2001).

[23] J.C.H. Fung, J.C.R. Hunt, N.A. Malik, and R.J. Perkins, J. Fluid Mech. **236**, 281 (1992).

[24] F. Nicolleau and J.C. Vassilicos, Phys. Rev. Lett. **90**, 024503 (2003).

[25] N.A. Malik and J.C. Vassilicos, Phys. Fluids **11**, 1572 (1999).

[26] B. Shraiman and E. Siggia, C. R. Acad. Sci., Ser. IIb: Mec., Phys., Chim., Astron. **321**, 279 (1995).

[27] J.C.H. Fung and J.C. Vassilicos, Phys. Rev. E **57**, 1677 (1998).

[28] J. Davila and J.C. Vassilicos, e-print physics/0207108.

[29] G. Boffetta and A. Celani, Physica A **280**, 1 (2000).

[30] P.K. Yeung, Phys. Fluids **6**, 3416 (1994).